Searching for the Evidence of the Galactic Dark Matter Halo Based on CNN Image Processing for Gravitational Lens images

Minsu Ko*

Department of Physics, Korea Advanced Institute of Science and Technology (KAIST) and Institute for Basic Science/Center for Axion and Precision Physics Research (IBS/CAPP)

In the field of modern experimental cosmology, understanding dark matter through observation remains a crucial challenge. Gravitational lensing is a vital technique for investigating dark matter properties, and the dominant λCDM model suggests that galaxies are embedded within dark matter halos. Recently, with advances in machine learning, particularly Convolutional Neural Networks (CNNs), there has been an increased interest in applying these techniques to analyze observational astronomical image data. The central focus of the research was the utilization of CNNs to examine gravitational lensing effects in simulated images caused by galaxies and their surrounding dark matter halos. The CNNs were adept at predicting physical properties of lens galaxies when trained with these images. While the models could not precisely estimate the Navarro-Frenk-White (NFW) dark matter halo distribution, they were capable of reliably detecting its presence around galaxies. Finally, the trained CNN was employed to analyze images from the Hubble Space Telescope (HST) taken during the COSMOS survey, concluding that most observed galaxies were indeed surrounded by dark matter halos.

I. INTRODUCTION

The concept of dark matter was first proposed in 1933 by Fritz Zwicky, who discovered that galaxies in the Coma cluster could not be held together solely by their visible mass and introduced the idea of dark matter to account for this gravitational anomaly [1]. Today, the prevailing model in cosmology is the λCDM framework, which emphasizes the importance of cold dark matter and the accelerating expansion of the universe driven by dark energy. Although the existence of dark matter and its crucial role in the evolution of the universe are widely accepted, its nature remains unknown, which makes studying its properties, origins, and distribution a key focus in modern astrophysics and astronomy. Broadly, dark matter experiments fall into two categories. The first is direct detection, where highly sensitive detectors search for specific dark matter candidates such as Axion [2] and WIMPs [3]. The second category involves indirect methods for inferring the presence and characteristics (such as distribution and density) of dark matter. These methods include cosmological observations such as measuring the rotational velocities of galaxies [4] and observing gravitational lens effects [5], which has been regarded as one of the most useful windows to the dark matter [6]. More recently, the Lenstronomy software that simulates gravitational lens effect has been developed [7] and enabled researchers to estimate the physical parameters of gravitational lens phenomena through computational simulations with various lens effect models. A notable achievement of this software is its compatibility with machine learning networks. These networks can be trained to recognize properties of simulated images [8], further enhancing its effectiveness.

The λCDM model posits that galaxies are embedded within dark matter halos [9]. Given their massive nature, these halos can produce gravitational lens effects, although their magnitude is relatively weak [10]. In this study, we used convolutional neural networks (CNNs) to analyze gravitational lensing effects caused by Navarro-Frenk-White (NFW) dark matter halos. The NFW dark matter halo is one of the ideal model for the mass distribution of dark matter halos, which was suggested from N-body simulations in late 20th-century [11]. Lenstronomy simulation with proper physical parameters provided sufficient amount of images of gravitational lens effect used for training, validation, and performance estimation of CNNs. At the first stage of the research, a CNN was trained by gravitational lens images created by Lenstronomy simulations and it was represented that a neural network can be trained and predict physical parameters of galaxies in at least SIE (Singular Isothermal Ellipsoid) and EPL (Elliptical Power Law) lens effect model. Subsequently, the CNN underwent training using gravitational lens images containing NFW dark matter halos, with the objective of predicting the physical parameters associated with the mass distribution and shape of these dark matter halos. However, it was determined that the CNN was incapable of accurately anticipating the physical parameters of the dark matter halos. Despite this limitation, the CNN could still discern the presence of dark matter halos in the images, even if their actual distribution was not extractable. Finally, by training a CNN with single-galaxy images that included (and do not include) dark matter halos, I achieved a binary classification precision of 0.75 for detecting the presence of dark matter halos. This neural network suggested that about 99.5% of galaxies from COSMOS survey from HST (Hubble Space Telescope) have dark matter halo around them. This research offers one of the most simplest combination of gravitational lens simulation and neural network methodology for the dark matter research. Also, it suggests that the simple framework in this research is enough to predict the existence of dark matter halos in non-irregular galaxies.

II. METHODOLOGY

In this section, the way to simulate gravitational lensing effect images using Lenstronomy is explained. Also, the structure of data set and CNNs is illustrated.

* komin0310@kaist.ac.kr

A. Lenstronomy Simulations

1. Strong Lensing Simulations

Basically, there are tons of lens effect models in Lenstronomy. In this research, Singular Isothermal Ellipsoid (SIE) and Elliptical Power Law (EPL), and external shear lens models were used to generate strong lensing effects. Additionally, NFW model was used to generate additional lensig effect caused by the presence of dark matter halos. In order to use specific lens effect model such as SIE and EPL, the names of the lensing effect models should be declared in the lens model list and appropriate parameters should be assigned. By providing several model names and sets of parameters, it is possible to combine multiple models together. Theoretically, each model can be specified its dimensionless parameter κ. It represents how the light is bent by the lens galaxy. SIE and EPL profiles are written as following. EPL requires one more parameter, the power-law slope γ [12].

$$\kappa(x,y) = \frac{1}{2}\left(\frac{\theta_E}{\sqrt{qx^2+y^2/q}}\right) \tag{1}$$

$$\kappa(x,y) = \frac{3-\gamma}{2}\left(\frac{\theta_E}{\sqrt{qx^2+y^2/q}}\right)^{\gamma-1} \tag{2}$$

The NFW dark matter halo lens model require 4 parameters; the scale radius (R_s) of the dark matter halos, deflection angle at scale radius, and two center coordinates. R_s mainly determines the mass distribution of the halo as following.

$$\rho(r) = \frac{\rho_0}{\frac{r}{R_s}\left(1+\frac{r}{R_s}\right)^2} \tag{3}$$

In order to generate a gravitational lensing effect image with certain models, observation conditions and physical parameters of the gravitational lensing effect and galaxies should be assigned. It also includes a pixel size (which is fixed as 64 by 64 in this research) and arseconds per pixel. In principle, one image consists of two galaxies: source and lens. The galaxies have 7 parameters respectively; amplitude of light, center coordinates, eccentricities, and two parameters related to the Sérsic profile [14]. The lensing effect parameters differ in model by model but generally includes Einstein radius, center coordinates, and eccentricities. Also, the shear model was applied that accounts the additional lensing effect caused by external gravitational effect except for the lens galaxy. All physical parameters were generated from proper random distributions depicted in TABLE I, to simulate realistic images. Following this, lens model, source model, and lens light model classes are set up based on the randomly defined parameters. The image data and PSF classes are then created by the pre-provided data and PSF variables. With these elements in place, the simulated lensed image can be generated using the ImageModel class by passing the data classes, lens models, source models, and lens light models. To make the simulation more realistic, noise, such as Poisson and background noise, is added to the results. Finally, the simulated image containing noise is generated. Example images generated by 3 models are shown in FIG 1.

Random Distributions of Parameters

Component	Distribution
Lensing effect	
Einstein radius ($''$)	1
Power-law slope (for EPL)	$\gamma_{\text{lens}} \sim \mathscr{N}_{log}(\mu: 0.7,\ \sigma: 0.1)$
x-coordinate lens center ($''$)	$x_{\text{lens}} \sim \mathscr{N}(\mu: 0,\ \sigma: 0.102)$
y-coordinate lens center ($''$)	$y_{\text{lens}} \sim \mathscr{N}(\mu: 0,\ \sigma: 0.102)$
x-direction eccentricity	$e_1 \sim \mathscr{N}(\mu: 0,\ \sigma: 0.2)$
xy-direction eccentricity	$e_2 \sim \mathscr{N}(\mu: 0,\ \sigma: 0.2)$
External shear	
Shear modulus	$\gamma_{\text{ext}} \sim \mathscr{N}_{log}(\mu: -2.73,\ \sigma: 1.05)$
Orientation angle	$\phi_{\text{ext}} \sim \mathscr{U}(-\frac{\pi}{2}, \frac{\pi}{2})$
Galaxies	
Amplitude (Lens)	$\mathscr{U}(1, 15)$
Amplitude (Source)	$\text{Amplitude}_{\text{lens}} \times \mathscr{U}(0, 1)$
Sérsic radius	$R_{\text{src}} \sim \mathscr{N}_{log}(\mu: -0.7,\ \sigma: 0.4)$
Sérsic index	$n_{\text{src}} \sim \mathscr{N}_{log}(\mu: 0.7,\ \sigma: 0.4)$
x-coordinate center ($''$)	$x_{\text{lens}} \sim \mathscr{N}(\mu: 0,\ \sigma: 0.102)$
y-coordinate center ($''$)	$y_{\text{lens}} \sim \mathscr{N}(\mu: 0,\ \sigma: 0.102)$
x-direction eccentricity	$e_1 \sim \mathscr{N}(\mu: 0,\ \sigma: 0.2)$
xy-direction eccentricity	$e_2 \sim \mathscr{N}(\mu: 0,\ \sigma: 0.2)$
NFW dark matter halo	
Scale radius	$R_s \sim \mathscr{U}(10, 100)$
Deflection angle at scale radius	$\alpha_{\text{NFW}} \sim \mathscr{N}_{log}(\mu: 0,\ \sigma: 0.1)$
x-coordinate center ($''$)	$x_{\text{NFW}} \sim \mathscr{N}(\mu: 0,\ \sigma: 0.102)$
y-coordinate center ($''$)	$x_{\text{NFW}} \sim \mathscr{N}(\mu: 0,\ \sigma: 0.102)$

TABLE I: The proper random distributions for each parameter in image simulations. Most of the distributions were suggested by [13]. $\mathscr{U}$, $\mathscr{N}$ stand for the uniform distribution and the normal distribution, respectively.

2. Single Galaxy Simulations

Although the Lenstronomy is a gravitational lensing effect simulator, it is possible to simulate an image of a single galaxy utilizing it by simply removing the lens galaxy settings. In the single galaxy simulations, power law galaxy model was used. In order to train a CNN to determine the presence or absence of a dark matter halo, images of galaxies with NFW dark matter halos were also simulated. In this case, there is no strong gravitational lensing effect, but weak lensing effect by the dark matter halo exists. The observation settings are different in strong lensing simulations and single galaxy simulations since single galaxy simulations were designed to imitate the COSMOS survey data. Example images are depicted in FIG 1.

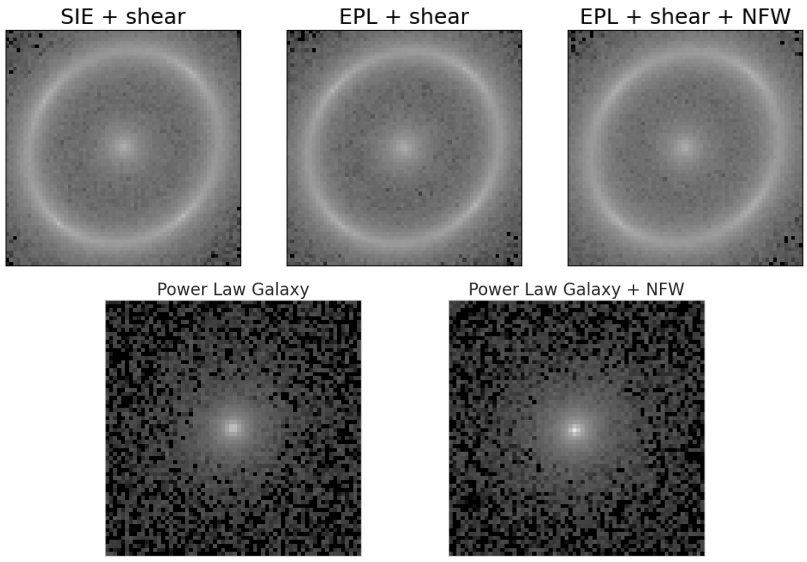

FIG. 1: Example images of strong gravitational lensing effects by the three lens models with an ideal parameter setting.

B. Dataset Composition

The data sets are composed of simulated images and labels. With SIE and EPL models combined with external shear, CNNs predicted the physical parameters of the lens galaxies. In this case, the shape of the labels is 6 by 1 numpy array which include two Sérsic parameters, two center coordinate values, and two eccentricities mentioned in TABLE I. The CNNs were supposed to predict the distribution of NFW dark matter when they worked with the EPL+shear+NFW model. Labels were 4 by 1 numpy array including scale radius, deflection angle at scale radius, and two center coordinate values of NFW dark matter halos shown in TABLE I also. At the binary classification tasks where CNNs predicted the presence (or absence) of the dark matter halo in the system, one-hot vector labels were used for the softmax classification. Images generated by the model without dark matter halos were labeled as [1,0] while images with dark matter halos were labeled as [0,1].

For all tasks, 80,000 images were used for training, 20,000 images were assigned for validation during the training, and 10,000 images were used as test data evaluating the performance of the models after training. As criterion, MSE loss was used for the parameter predictions and Cross Entropy loss was used for the binary classifications. Training loss and validation loss was traced during the training. Especially in the binary classifiaction tasks, training and validation accuracy was recorded.

C. CNN Establishment

CNNs with various hyperparameter settings were tested in pytorch framework. It turned out that utilizing 3 convolution layers and 2 linear layers is one of the best settings in terms of performance and training time. The Cosine Annealing Warm Restarts learning rate schedulers were also implemented for the first three tasks. Especially for the last task (prediction of NFW dark matter halo in single galaxy images), Cosine Annealing Warm Up Restart [15] scheduler was utilized. One convolution layer consists of 2D convolution operation, PReLU activation, and max pooling. Stride and padding of 2D convolution was fixed as 1, while stride and kernel size of max pooling was fixed as 2 for all cases. The dimension of the final output depends on the labels of the image data set. The detail setting for the CNNs are described in TABLE II. Also, the whole schematic of the CNNs is shown in FIG 2.

CNN Settings for Each Task

Prediction	Kernel size of Conv2D	Fully Connected layers	Output
Lens Galaxy Parameters	3	Linear $\rightarrow$ DO $\rightarrow$ ReLU $\rightarrow$ Linear	6 by 1
NFW Parameters	3	Linear $\rightarrow$ DO $\rightarrow$ ReLU $\rightarrow$ Linear	4 by 1
Presence of NFW (Strong lensing)	3	Linear $\rightarrow$ DO $\rightarrow$ ReLU $\rightarrow$ Linear $\rightarrow$ softmax	2 by 1
Presence of NFW (Single galaxy)	5	Linear $\rightarrow$ DO $\rightarrow$ ReLU $\rightarrow$ Linear $\rightarrow$ softmax	2 by 1

TABLE II: The detailed settings of CNNs for each prediction task. DO stands for DropOut with 0.5 probability.

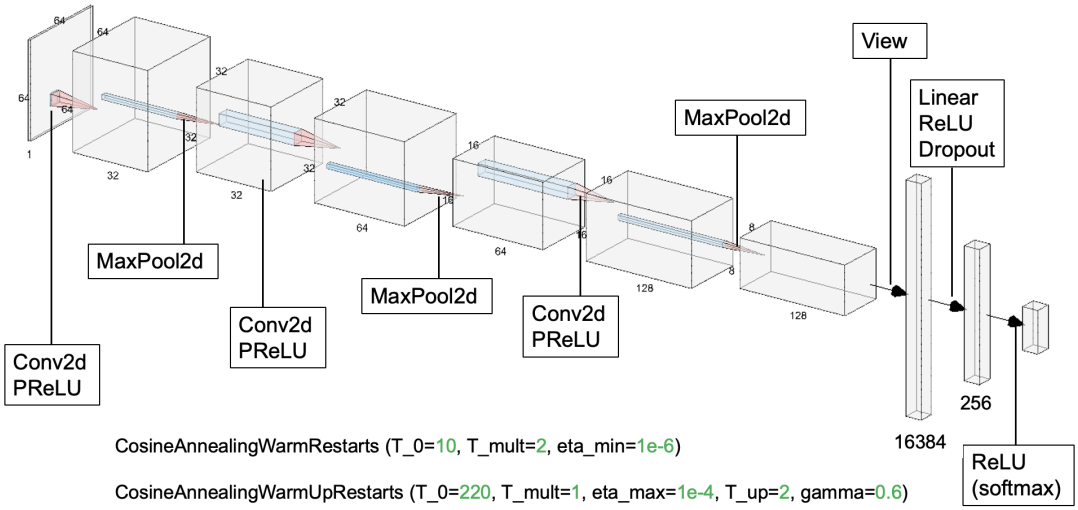

FIG. 2: A whole schematic of the CNNs. Kernel size, output dimension, and learning rate schedulers differ by tasks. Especially right before the output, softmax activation was used for the binary classification tasks.

III. SIMULATION RESULT & APPLICATION

A. Strong Lensing Simulations

1. *Parameter Prediction*

As mentioned, there are several parameters in labels. The range of values of each parameter vary: for example, R_s of NFW model is from 10 to 100, while the center coordinate of galaxies and dark matter halos are smaller than 1. To reduce the difference between them and also improve the performance of CNNs, parameters with large values were reduced by being divided by certain value. During the training with the SIE + shear model and the EPL + shear model images, MSE validation loss was below 0.002 after 100 epochs, which means successful training. However, validation loss of the training by EPL + shear + NFW model images started diverging after certain epoch. Therefore, the evaluation of the model was performed only after 40 epochs.

The MSE error between the prediction of the CNNs and label values for each parameters in test data set was obtained after the training. The results are shown in FIG 3. It shows the Sérsic parameters are harder to predict compared to the center coordinate values of the lens galaxies. Also, one notable point is that the scale of MSE error from EPL + shear + NFW model is much larger than ones from others. It implies that the training with images from EPL + shear + NFW model was unsucessful and the CNN cannot predict the parameters of NFW dark matter halo. In order to observe the performance of the CNNs more directly, the agreement plots were plotted as depicted in FIG 4. They have label values and prediction values at x-axis and y-axis, respectively. Thus, if the model perfectly predict the parameters, all points are aligned along the $y = x$ line. It is obvious that the CNNs well predicted the lens galaxy parameters in the SIE + shear and EPL + shear models. However, predictions about NFW dark matter halo never align along the $y = x$ line, which means the CNN cannot tell about the distribution of dark matter halos.

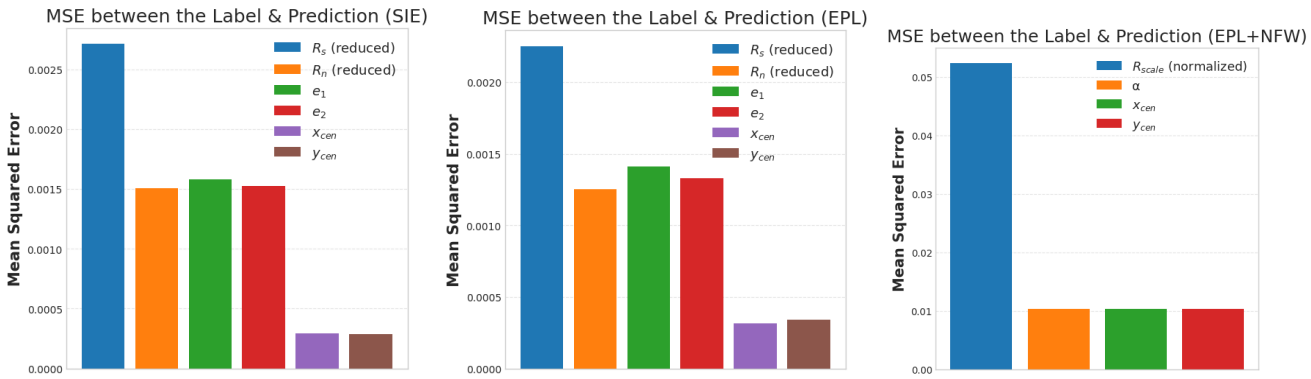

FIG. 3: MSE error between the predicition of the CNNs and label values of test data set for each parameter and model.

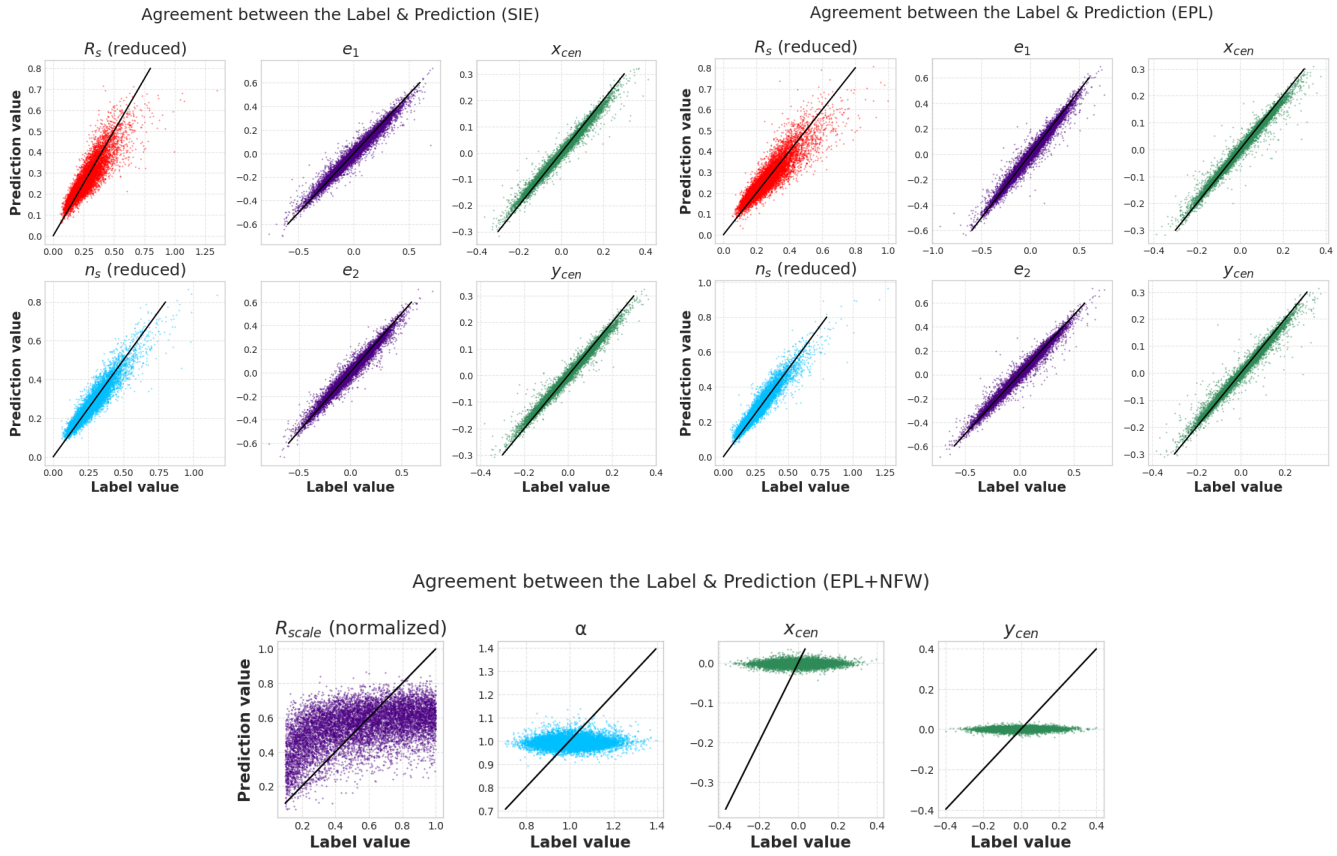

FIG. 4: The agreement plots for the lens galaxy parameters and the NFW parameters of each model.

2. *NFW dark matter halo Detection*

Especially for this binary classification task, simulated images from two different models were implemented with one-hot vector labels in the data sets. 40,000 images from EPL + shear and another 40,000 images from EPL + shear + NFW composed the training data set. Similarly, 10,000 images from each model consisted the validation data set together, and in the test data set, 5,000 images from the models were used. Only after 27 epochs, the validation accuracy achieved 0.73. Especially in the single galaxy simulations, all values in pixels were normalized to improve the performance of the CNN. The evaluation metrics from the test data set is shown in TABEL III. In the evaluation metric calculations, the positive is presence of NFW dark matter halos and the negative corresponds to absence of them.

Evaluation Metrics of Binary Classifications

	Strong Lensing	Single Galaxy
Metric	value	value
Accuracy	0.733	0.694
Precision	0.750	0.748
Recall	0.700	0.585
F1 score	0.724	0.656

TABLE III: The evaluation metrics of the binary classifications (NFW dark matter halo detection) in the strong lensing simulation and the single galaxy simulation.

B. Single Galaxy Simulations

Similarly, half of images in data sets was from power law galaxy model and another half was created by power law galaxy + NFW model. The validation accuracy was above 0.7 after 62 epochs. The evaluation metrics from the test data set is shown in TABEL III also.

The overall performance was better in strong lensing simulations. It is natural because the hyperparameters and the learning rate scheduler differ in two models and image structures of the strong lensing simulation and single galaxy simulation also differ obviously. Additionally, the observation settings (noise, exposure time, and arcseconds per pixel) are different in strong lensing simulations and single galaxy simulations. It is because single galaxy simulations were designed to imitate the COSMOS survey data, which consist of images of real galaxies. This difference may have affected the performance of the models. Nevertheless, the precision of models were similar and actually the highest metric. This high precision indicates that the models excel at making accurate positive predictions (presence of dark matter halo).

C. Application to COSMOS Survey Data

The Cosmic Evolution Survey (COSMOS) survey was performed by the Hubble Space Telescope (HST). It encompasses a sufficiently large area that it can address the coupled evolution of LSS, galaxies, star formation, and AGNs [16]. A 4.4 GB fits file includes about 29000 images [17] which are able to be converted to numpy arrays directly through the astropy package. Although the arcseconds per pixel of images in a file is fixed as 0.03 $''$, the size of images varies. First of all, too large images (over 80 pixels per line), too small images (below 50 pixels per line), and too bright images (maximum value of a pixel is over 2) were rejected. This pre-process filtered 3707 images out of 29062. Also, the normalization was performed just as the single galaxy simulation images.

Finally, the normalized COSMOS survey images went through the CNN trained by the single galaxy simulations. It predicted that 3689 galaxies out of 3707 (about 99.5%) have dark matter halos around them. It was a desirable result which agrees with λCDM, since it asserts that almost every galaxy in the universe has a dark matter halo surrounding it. FIG 5 shows the 18 images of galaxies that the CNN determined do not contain dark matter halos. Most of them seem to be irregular galaxies. It is obviously because the CNN is trained only by images of galaxies obeying the power law, but not irregular galaxies. The result cannot be trusted perfectly because power law galaxies and NFW dark matter halo model are ideal cases, and the accuracy and precision of the CNN is far from perfect. Despite these limitations, these results suggest that almost all galaxies are nestled in dark matter halos.

IV. CONCLUSION

In this research, CNNs established in the pytorch framework were trained by strong lensing simulation images and images from single galaxy with (and without) weak lensing effect caused by NFW dark matter halos, which were generated by Lenstronomy package. Especially the CNN trained by single galaxy images predicted the presence of dark matter halos in real observation images from COSMOS survey. This research demonstrates the capacity of CNNs to be trained on strong gravitational lensing effect images and extract physical parameters of lens galaxies. Although unable to predict the distribution of NFW dark matter halos in strong lensing images, CNNs successfully detected their presence in both strong lensing images and images from single galaxy simulation. Remarkably, the CNN trained by single galaxy simulations indicated that approximately 99.5% of galaxies in the COSMOS survey are situated within dark matter halos. While this research is limited by its reliance on idealized galaxy and dark matter halo models, as well as the accuracy of neural networks, it highlights the compatibility of CNNs and Lenstronomy strong lensing effect simulations. Consequently, this study suggests that it is feasible to capture evidence of galactic dark matter halo existence using CNNs and simulated weak gravitational lensing images of single galaxies and NFW dark matter halos.

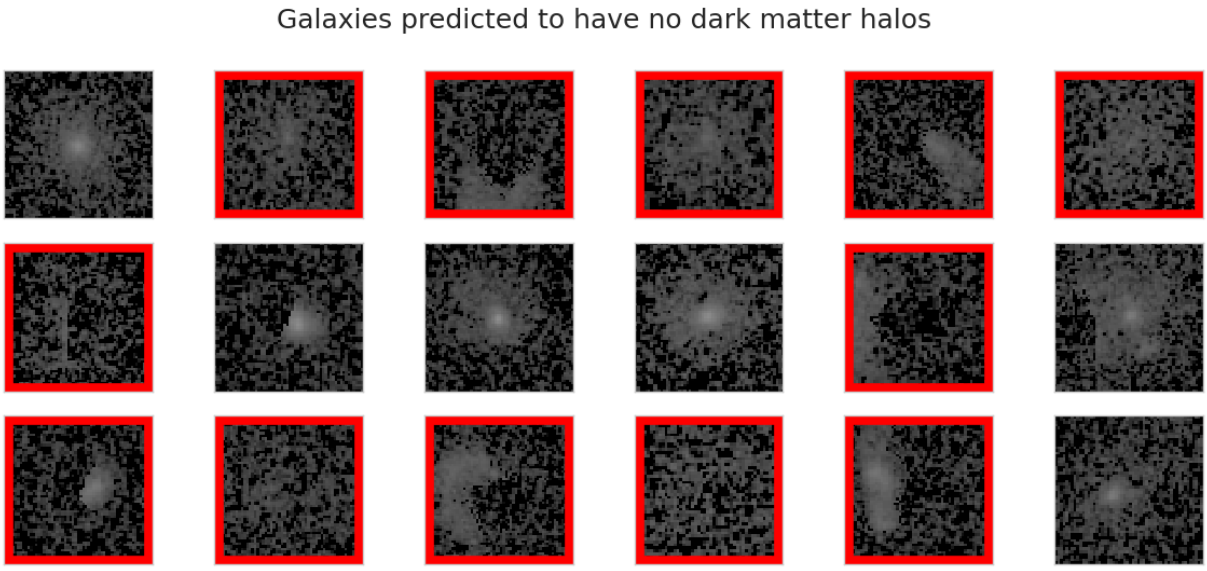

FIG. 5: The images of galaxies that the CNN determined do not contain dark matter halos. Images surrounded by red rectangles are suspected to be images of irregular galaxies.

[1] F. Zwicky, Republication of: The redshift of extragalactic nebulae, General Relativity and Gravitation **41**, 207 (2009).

[2] B. Brubaker, L. Zhong, Y. Gurevich, S. Cahn, S. Lamoreaux, M. Simanovskaia, J. Root, S. Lewis, S. Al Kenany, K. Backes, *et al.*, First results from a microwave cavity axion search at 24 μ ev, Physical review letters **118**, 061302 (2017).

[3] D. S. Akerib, H. Araújo, X. Bai, A. Bailey, J. Balajthy, S. Bedikian, E. Bernard, A. Bernstein, A. Bolozdynya, A. Bradley, *et al.*, First results from the lux dark matter experiment at the sanford underground research facility, Physical review letters **112**, 091303 (2014).

[4] V. C. Rubin and W. K. Ford Jr, Rotation of the andromeda nebula from a spectroscopic survey of emission regions, The Astrophysical Journal **159**, 379 (1970).

[5] R. Massey, T. Kitching, and J. Richard, The dark matter of gravitational lensing, Reports on Progress in Physics **73**, 086901 (2010).

[6] R. S. Ellis, Gravitational lensing: a unique probe of dark matter and dark energy, Philosophical Transactions of the Royal Society A: Mathematical, Physical and Engineering Sciences **368**, 967 (2010).

[7] S. Birrer, A. J. Shajib, D. Gilman, A. Galan, J. Aalbers, M. Millon, R. Morgan, G. Pagano, J. W. Park, L. Teodori, N. Tessore, M. Ueland, L. V. de Vyvere, S. Wagner-Carena, E. Wempe, L. Yang, X. Ding, T. Schmidt, D. Sluse, M. Zhang, and A. Amara, lenstronomy ii: A gravitational lensing software ecosystem, Journal of Open Source Software **6**, 3283 (2021).

[8] H. Khachatryan, On machine learning search for gravitational lenses, arXiv preprint arXiv:2104.01014 (2021).

[9] R. H. Wechsler and J. L. Tinker, The connection between galaxies and their dark matter halos, Annual Review of Astronomy and Astrophysics **56**, 435 (2018).

[10] E. van Uitert, H. Hoekstra, T. Schrabback, D. G. Gilbank, M. D. Gladders, and H. Yee, Constraints on the shapes of galaxy dark matter haloes from weak gravitational lensing, Astronomy & Astrophysics **545**, A71 (2012).

[11] J. F. Navarro, The structure of cold dark matter halos, in *Symposium-international astronomical union*, Vol. 171 (Cambridge University Press, 1996) pp. 255–258.

[12] N. Tessore and R. B. Metcalf, The elliptical power law profile lens, Astronomy & Astrophysics **580**, A79 (2015).

[13] S. Wagner-Carena, J. W. Park, S. Birrer, P. J. Marshall, A. Roodman, R. H. Wechsler, L. D. E. S. Collaboration, *et al.*, Hierarchical inference with bayesian neural networks: An application to strong gravitational lensing, The Astrophysical Journal **909**, 187 (2021).

[14] J. Sérsic, Influence of the atmospheric and instrumental dispersion on the brightness distribution in a galaxy, Boletin de la Asociacion Argentina de Astronomia La Plata Argentina **6**, 41 (1963).

[15] J. Kim, Pytorch learning rate scheduler (2020), accessed: 2023-06-06.

[16] N. Scoville, H. Aussel, M. Brusa, P. Capak, C. M. Carollo, M. Elvis, M. Giavalisco, L. Guzzo, G. Hasinger, C. Impey, *et al.*, The cosmic evolution survey (cosmos): overview, The Astrophysical Journal Supplement Series **172**, 1 (2007).

[17] R. Mandelbaum, C. Lackner, A. Leauthaud, and B. Rowe, Cosmos real galaxy dataset (2012), accessed: 2023-06-07.